

Ultralow-power all-optical wavelength conversion in a silicon-on-insulator waveguide based on a heterogeneously integrated III-V microdisk laser

Liu Liu,^{1,a)} Joris Van Campenhout,^{1,b)} Günther Roelkens,¹ Dries Van Thourhout,¹ Pedro Rojo-Romeo,² Philippe Regreny,² Christian Seassal,² Jean-Marc Fédéli,³ and Roel Baets¹

¹Photonics Research Group, IMEC/Ghent University, St-Pietersnieuwstraat 41, 9000 Ghent, Belgium

²Institut des Nanotechnologies de Lyon, Université de Lyon, INL-UMR5270, CNRS, Ecole Centrale de Lyon, Ecully F-69134, France

³CEA-LETI, Minatec 17 rue des Martyrs, 38054 Grenoble, France

(Received 23 June 2008; accepted 14 July 2008; published online 13 August 2008)

Ultralow-power all-optical wavelength conversion is presented for a silicon-on-insulator wire waveguide with a heterogeneously integrated III-V microdisk laser. The principle relies on the suppression of natural lasing from the microdisk laser by an external injection. No probe beam is needed in this configuration. Static wavelength conversion with a control power of $6.4 \mu\text{W}$ or even lower is achieved. The resonance and gain provided by the microdisk cavity are at the origin of such low control power. Dynamically, wavelength conversion using a 5 Gbps non-return-to-zero bit sequence is demonstrated in the proposed device. © 2008 American Institute of Physics. [DOI: 10.1063/1.2967338]

Silicon photonics, especially those based on the silicon-on-insulator (SOI) material system, have attracted considerable research interest.¹ The high refractive index contrast between the core and cladding materials results in a tightly confined light field, which leads to a high-density integration of devices. All-optical signal processing, e.g., wavelength conversion, has been demonstrated recently with a single SOI waveguide² or a SOI ring cavity^{3,4} based on either the free-carrier dispersion or the four-wave mixing effect. Although the high-index-contrast provided by these structures is expected to enhance the nonlinear response, milliwatts (or more) of control power are still required due to the relatively weak coefficients of these effects in silicon.

In this paper, we introduce an all-optical wavelength converter based on a heterogeneous III-V/SOI platform. The proposed device is composed of a III-V microdisk laser (MDL) integrated on a SOI wire waveguide.⁵ Different from the popular pump-probe scheme, only a single beam—the input control signal—is needed in this configuration. The working principle is based on the fact that the natural lasing from the MDL can be suppressed when an external control beam is injected into the microdisk cavity. Therefore, the information carried on the injected beam will be inversely transferred to the natural lasing wavelength of the MDL. Because of the gain and resonance provided by the microdisk cavity for the injected beam, wavelength conversion with ultralow control power (of several microwatts) is achieved with the proposed device.

Figure 1 shows the sketch of the experimental setup. The employed MDL has a diameter of $7.5 \mu\text{m}$. The underlying SOI wire waveguide is terminated with grating couplers at both ends for light access from fibers.⁶ For wavelength conversion, an external control laser was injected into the MDL,

which is direct current (dc) biased, through the grating coupler at one end of the SOI waveguide. The total output light was collected at the other end of the waveguide. The residual control beam was then blocked by a bandpass filter, and only the natural lasing wavelength from the MDL was detected. For dynamic measurements, a modulator (with a speed up to 10 GHz) was employed to modulate the control laser beam, and an erbium-doped fiber amplifier (EDFA) was inserted before the bandpass filter.

The corresponding light-current (L - I) curve (fiber-coupled power) of the MDL under continuous bias is plotted in Fig. 2. The threshold current is 1.1 mA, and the peak fiber-coupled power is $2.0 \mu\text{W}$. Accounting for a grating coupler efficiency of 25%, the actual lasing power in the SOI waveguide is estimated to be $8.0 \mu\text{W}$. From the output spectrum (inset of Fig. 2), we find that the MDL is lasing in a single mode. The side-mode suppression ratio is ~ 20 dB. A clear rollover of the L - I curve at a high current can be seen due to the significant thermal resistance of the device.⁷ Further increasing the bias current results in the lasing wavelength, switching from mode 1 to mode 2, one free-spectral-range away at the longer wavelength side. Correspondingly, we see a drop in the fiber-coupled lasing power around 4.2

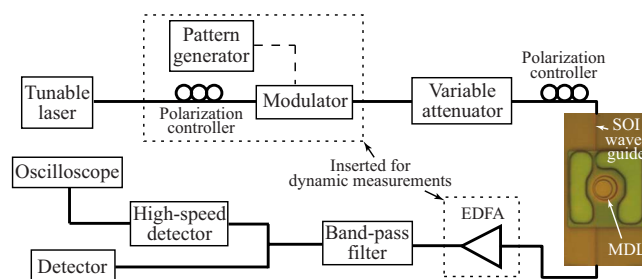


FIG. 1. (Color online) Experimental setup and microscope picture of the MDL.

^{a)}Electronic mail: liu@intec.ugent.be.

^{b)}Present address: IBM T. J. Watson Research Center, 1101 Kitchawan Rd., Yorktown Heights, NY 10598, USA.

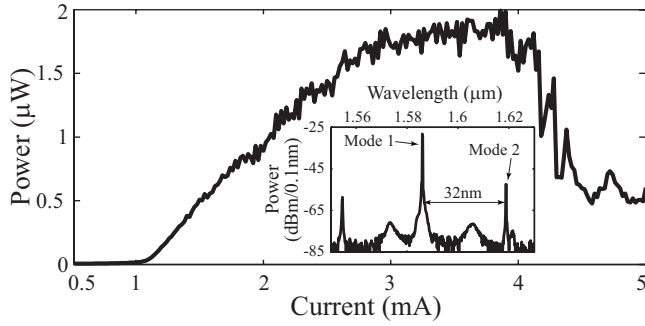


FIG. 2. L - I curve of the MDL. Inset shows the output spectrum at 3.5 mA bias.

mA due to the different coupling efficiencies at the grating coupler for these two modes.

The wavelength conversion was first measured under static conditions. The MDL was biased at 3.5 mA. The optical power carried on the natural lasing wavelength, i.e., mode 1, was recorded while scanning the wavelength of the control beam around that of mode 2. The results are shown in Fig. 3(a). A clear drop in power in mode 1 can be found when the control beam is at resonance with mode 2. The power dip is almost symmetrical along the central wavelength at a low injection power. A suppression ratio of ~ 20 dB was achieved with only $6.4 \mu\text{W}$ control power in the SOI waveguide. As the control power increases, this dip becomes more and more asymmetrical, and a hysteresis loop emerges at a higher injection (19.2 μW). To analyze these measured results, a rate-equation based model is employed as⁸

$$\frac{dN}{dt} = R - \frac{N}{\tau_e} - G_1 v_g S_1 - G_2 v_g S_{inj}, \quad (1)$$

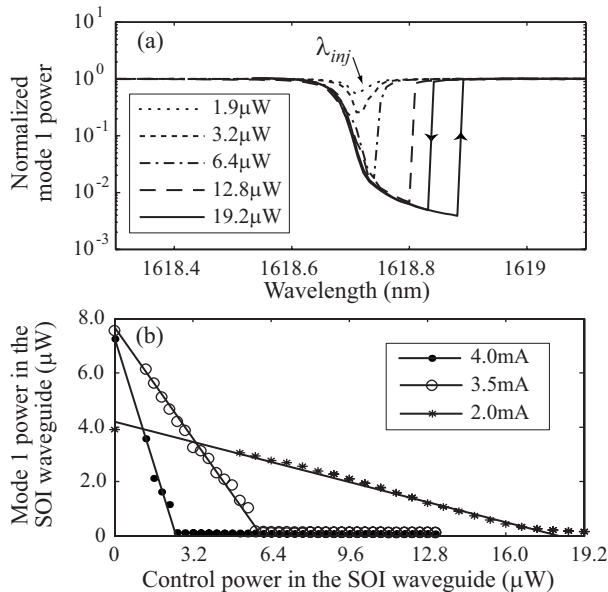


FIG. 3. Static measurement results. (a) Normalized mode 1 power as a function of the control laser wavelength. Parameters are the control power in the SOI waveguide. The wavelength used for the dynamic measurements below is marked as λ_{inj} . (b) Mode 1 power as a function of the control power. Parameters are the bias current. The control laser is at the same wavelength as mode 2. The solid lines are the theoretical fittings according to Eq. (4).

$$\frac{dS_1}{dt} = G_1 v_g S_1 - \frac{S_1}{\tau_p}. \quad (2)$$

Here, we ignore the spontaneous emission and only consider the case that the wavelength detuning between the injected control laser and mode 2 is zero. In the above equations, N is the carrier number. S_1 is the photon number of mode 1. It is proportional to the detected optical power. R is the pumping rate proportional to the bias current. v_g is the group velocity. τ_e is the carrier lifetime. τ_p is the photon lifetime defined as $\{v_g[\alpha_i - \ln(1-\kappa)/L]\}^{-1}$, where α_i is the total internal loss, L is the periphery of the microdisk cavity, and κ is the power coupling coefficient between the microdisk and the waveguide. G_1 and G_2 are the mode gains for modes 1 and 2, respectively. S_{inj} is the injected photon number in the microdisk cavity. It is proportional to the injected control power in the SOI waveguide P_{inj} , as $S_{inj} = \xi \times P_{inj}$, where ξ is a coefficient, which takes into account the resonance and amplification in the cavity,^{8,9}

$$\xi = \frac{\kappa[e^{(G_2 - \alpha_i)L} - 1]}{E_p v_g (G_2 - \alpha_i) [1 - \sqrt{1 - \kappa e^{(G_2 - \alpha_i)L/2}}]^2}, \quad (3)$$

where E_p is the photon energy of the control beam.

Under static conditions, the MDL is lasing at mode 1 when no control power is injected. In this case, the gain is clamped at the threshold and $G_2 < G_1 = (v_g \times \tau_p)^{-1}$. From Eq. (1), we can find that as the power of the control laser increases, the photon number S_1 of mode 1 will first decrease correspondingly, while the carrier number and the mode gain remain unchanged. Further increasing the control power will make S_1 drop to zero, and the lasing wavelength of the MDL will shift to mode 2 due to injection locking.¹⁰ The carrier number will also decrease in order to balance Eq. (1). This is the reason for the asymmetry of the dip as well as the hysteresis loop in Fig. 3(a). Further discussion of this injection locking effect is beyond the scope of this letter. It is also not included in the aforementioned model. Under static operation we derive the following relation between S_1 and P_{inj} from Eq. (1) (until S_1 reaches zero):

$$S_1 = \left(\frac{R}{G_1 v_g} - \frac{N}{G_1 v_g \tau_e} \right) - \frac{G_2}{G_1} \xi P_{inj}. \quad (4)$$

Equation (4) describes a simple linear function with a slope of $(G_2/G_1)\xi$. From Eq. (3), it can be easily found that this slope is actually a monotonic increasing function of G_2 . Therefore, the required control power can be further reduced by increasing G_2 . This can be readily achieved in the proposed devices by applying a higher bias current. As the current approaches the switching point of the L - I curve, the peak gain wavelength of the active material will redshift due to the thermal effect. Correspondingly, G_2 will also increase until it reaches the threshold condition $(v_g \times \tau_p)^{-1}$. In this case, the slope $(G_2/G_1)\xi$ approaches infinity. Figure 3(b) shows the measured power of mode 1 as a function of the injected control power at several bias conditions. As we can see, 2.5 μW control power is enough to shut off mode 1 when the current increases to 4.0 mA.

The dynamic results are shown in Fig. 4, where the control beam was modulated with a square wave signal at 500 MHz. The MDL was biased at 3.5 mA, and the peak control power was 6.4 μW . The resulting extinction ratio of the converted signal is ~ 15 dB, slightly less than the static re-

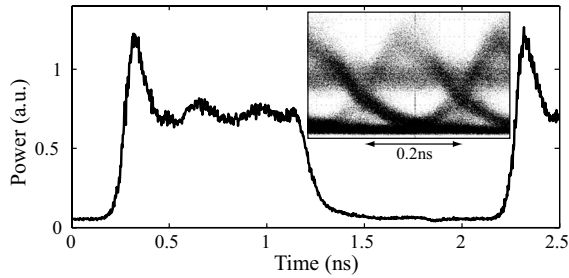


FIG. 4. Response of the converted signal under square wave input at 500 MHz. Inset shows the eye diagram of the converted signal for a 5 Gbps NRZ data pattern.

sult. This is due to the significant spontaneous emission from the EDFA. The rise and fall times are measured to be ~ 65 and ~ 130 ps, respectively, thanks to the much faster carrier dynamics as compared to the all-silicon approaches, where these transition times were originally reported to be in the order of nanoseconds.³ Although means have been introduced to improve the operation speed for the all-silicon devices by using, e.g., an embedded diode,¹¹ ion implantation,¹² or polycrystalline silicon,¹³ they come at the expense of either increasing the required control power or introducing extra optical losses. We also show, in Fig. 4, the output eye diagram for an input signal of 5 Gbps nonreturn to zero (NRZ) code with $2^{31}-1$ pseudorandom bit sequence. An open eye was obtained. However, the signal-to-noise ratio is still low due to the relatively weak lasing power of the MDL. This can be tackled by optimizing the MDL design for a higher output power.¹⁴ Dynamic analyses of Eqs. (1) and (2) reveal that the speed limit is given by the intrinsic relaxation oscillation frequency.¹⁰ Therefore, increasing the lasing power can also help to improve the operation speed. A 10 Gbps bit rate is expected if the output power reaches $100 \mu\text{W}$.¹⁴

In conclusion, all-optical wavelength conversion has been demonstrated in a SOI circuit based on an external injection to a heterogeneously integrated, dc biased III-V MDL. A general rate-equation based model has been presented to analyze the static results. ~ 20 dB extinction ratio of the converted beam has been achieved with a control

power of only $6.4 \mu\text{W}$ and even lower. Dynamic measurements have shown that the 5 Gbps bit rate is feasible with the present design. The proposed principle can also be applied for wavelength conversion from any resonant modes within the gain range of the active material to the natural lasing wavelength. However, a higher control power will be required as the injected wavelength moves further away from the natural lasing wavelength. The applicable wavelength range can be further expanded by including a tuning mechanism, e.g., a built-in heater.

L.L. acknowledges Interuniversity Attraction Poles (IAP) for a postdoctoral grant. G.R. acknowledges the Fund for Scientific Research-Flanders (FWO) for a postdoctoral grant. This work is supported partially by projects PICMOS and WADIMOS funded by EU.

¹W. Bogaerts, R. Baets, P. Dumon, V. Wiaux, S. Beckx, D. Taillaert, B. Luyssaert, J. Van Campenhout, P. Bienstman, and D. Van Thourhout, *J. Lightwave Technol.* **23**, 401 (2005).

²R. L. Espinola, J. I. Dadap, R. M. Osgood, Jr., S. J. McNab, and Y. A. Vlasov, *Opt. Express* **13**, 4341 (2005).

³Q. Xu, V. R. Almeida, and M. Lipson, *Opt. Lett.* **30**, 2733 (2005).

⁴A. C. Turner, M. A. Foster, A. L. Gaeta, and M. Lipson, *Opt. Express* **16**, 4881 (2008).

⁵J. Van Campenhout, P. Rojo-Romeo, D. Van Thourhout, C. Seassal, P. Regreny, L. Di Cioccio, J. M. Fedeli, C. Lagahe, and R. Baets, *Opt. Express* **15**, 6744 (2007).

⁶D. Taillaert, F. Van Laere, M. Ayre, W. Bogaerts, D. Van Thourhout, P. Bienstman, and R. Baets, *Jpn. J. Appl. Phys., Part 1* **45**, 6071 (2006).

⁷J. Van Campenhout, P. Rojo-Romeo, D. Van Thourhout, C. Seassal, P. Regreny, L. Di Cioccio, J. M. Fedeli, and R. Baets, *J. Lightwave Technol.* **25**, 1543 (2007).

⁸M. T. Hill, H. de Waardt, G. D. Khoe, and H. J. S. Dorren, *IEEE J. Quantum Electron.* **37**, 405 (2001).

⁹I. D. Henning, M. J. Adams, and J. V. Collins, *IEEE J. Quantum Electron.* **21**, 609 (1985).

¹⁰J. Hörer and E. Patzak, *IEEE J. Quantum Electron.* **33**, 596 (1997).

¹¹S. Preble, Q. Xu, B. Schmidt, and M. Lipson, *Opt. Lett.* **30**, 2891 (2005).

¹²M. Waldow, T. Plötzing, M. Gottheil, M. Först, J. Bolten, T. Wahlbrink, and H. Kurz, *Opt. Express* **16**, 7693 (2008).

¹³K. Preston, P. Dong, B. Schmidt, and M. Lipson, *Appl. Phys. Lett.* **92**, 151104 (2008).

¹⁴J. Van Campenhout, P. Rojo-Romeo, D. Van Thourhout, C. Seassal, P. Regreny, L. Di Cioccio, J. M. Fedeli, and R. Baets, *J. Lightwave Technol.* **26**, 52 (2008).